はじめに
Introduction

橋本博史
Hiroshi HASHIMOTO
順天堂大学附属順天堂越谷病院

血管炎は病理学的に血管壁の炎症として定義されるが，血管炎をきたす疾患は多い．血管炎を基礎としてもたらされる多種多様の臨床病態または疾患群は，血管炎症候群と総称される．これには血管炎を主病変とする独立した疾患(原発性)もあれば，他疾患に血管炎を伴う病態(続発性)も含まれる．それらの多くは原因不明であるが，多因子性疾患とされ，発症要因に遺伝的要因と環境因子，とくに感染症が重要視される．しかし，ヒトにおけるこれらの病因にかかわる因子の解析はきわめて複雑で困難なことが多い．この観点から，基礎的には血管炎症候群の病因・病態を解明するうえでヒトの血管炎と相同性をみるモデル動物の解析が重要である．

血管炎の発症には血管内皮細胞の傷害が重要視されるが，これには好中球，単球，リンパ球などの炎症性細胞，細胞の活性化や接着・浸潤に関与する種々のサイトカイン，接着分子，プロスタグランジン，ヒスタミンなどのメディエーターなど多くの因子が関与する．さらに，抗好中球細胞質抗体(ANCA)や抗血管内皮細胞抗体などの自己抗体も血管内皮細胞の傷害に関与する．臨床的には，疾患によって，人種や国，地域により発症率や有病率が異なることが指摘され，その要因の解明に向けて国際的共同研究も進められている．また，従来の非特異的免疫抑制療法に限界のあることも指摘され，生物学的製剤やγ-グロブリン療法，さらには血管再生を目的とした遺伝子導入などのあらたな治療法の展開もみられる．

本特集ではこれらの点を踏まえ，専門の方々に血管炎の基礎では血管炎の病因と病態形成に深くかかわる要因について，最近の知見を中心に解説していただき，血管炎の臨床では日常診療でしばしば経験する大型血管炎から細小血管炎に至るまでの原発性血管炎を中心に，診断と治療における最近の動向について解説をお願いした．

診る I-e

血管病変を診る
血管炎を診る

To examine the patients with vasculitis

橋本博史（順天堂大学附属順天堂越谷病院）

血管炎をきたす疾患は多い。血管炎を基盤としてもたらされる多種多様の臨床病態ないし疾患群は血管炎症候群とよばれる。これには，血管炎を主病変とする独立した疾患（原発性）もあれば，基礎疾患に血管炎を伴う病態（続発性）もみられる。前者における分類（表1）は，Jennetteら[1]により提唱されている。これは，障害を受ける血管の太さにより分類され，顕微鏡的多発血管炎（microscopic polyangiitis；MPA）は侵される血管の太さの違いと抗好中球細胞質抗体（antineutrophil cytoplasmic antibodies；ANCA）を認めることから，結節性多発動脈炎（polyarteritis nodosa；PN）より分離独立されている。一方，大型血管を侵す血管炎として高安動脈炎と側頭動脈炎があげられているが，その他続発性も含め表2のように多くの疾患が含まれる[2]。血管炎症候群に含まれる疾患の多くは原因が不明であるが，その発症には遺伝的要因と環境因子が重視される。本稿では，細動静脈炎をきたす疾患を除く原発性血管炎症候群を臨床的特徴を中心に述べる。

血管炎症候群の疫学

高安動脈炎は若年女性に発症するのに対し，側頭動脈炎は50歳以上の高齢者に発症する。川崎動脈病，Schönlein-Henoch紫斑病は小児にみられる。厚生省調査研究班による主な疾患の推計患者数と男女比を表3に示す[3]。

診断に有用な臨床的症候

薬剤やウイルス感染などはPN，皮膚白血球破砕性血管炎などの発症誘因

1342-6591/05/¥400/論文/JCLS

となる。気管支喘息を含むアレルギー体質や好酸球性肺炎，好酸球性腸炎などはアレルギー性肉芽腫性血管炎（allergic granulomatosis angiitis；AGA）の発症に先行して認められる。血管炎症候群の多くは，発熱，体重減少，関節痛，筋肉痛，筋力低下などの全身症状をみる。側頭動脈炎では，リウマチ性多発筋痛症や頭痛を伴う。紫斑，丘疹，水泡，じん麻疹様皮疹，網状皮斑などの皮膚症状は細小型血管炎を示唆する。結節性紅斑，皮下結節，皮膚潰瘍，四肢壊疽，多発性単神経炎，臓器梗塞などは中・小型血管炎を示唆する。他方，大型血管炎では，間欠性跛行，うっ血性心不全，高血圧，脳虚血症候，視力障害などをみる[2]（表4）。腎臓は多くの疾患で標的臓器となり，糸球体病変・半月体形成性腎炎から腎血管性病変によるものまでみられるが，前者は，MPAやWG（Wegener granulomatosis）など細小型血管炎をきたす疾患でみられやすく，後者はPN，さらには高安動脈炎など中・小動脈レベル以上の血管炎をきたす疾患でみられやすい。肺病変は，AGAとWGで認められるが，WGでは副鼻腔炎を含む上気道病変が先行する。大型血管炎では血管雑音の聴取が重要で，血圧や脈の左右差を認める以前より聴取される。

検査所見

検査所見では，通常，赤沈の亢進，CRP（C-reactive protein）陽性，白血球増多などの急性炎症所見をみる。AGAでは著しい好酸球の増加をみる。ANCAはMPA，AGA，WGなどで認められることが多く診断に有用である。血管造影は高安動脈炎の診断に重要な検査であるが，最近，冠動脈や大動脈弁閉鎖不全をみる心病変型の存在が指摘され，さらに日本では頻度は少ないが腹部大動脈に限局した病変をみる病型も存在する[4]。PNでは，小動脈瘤，血管壁の不整，狭窄を示す断節的陰影，閉塞などをみる。生検による組織学的所見は細・小・中型血管炎をみる疾患の診断に重要である。生検は，多くは病変部位が選ばれ，皮膚，筋，神

表1　血管炎の分類（文献1より改変引用）

大型血管炎
巨細胞性動脈炎（側頭動脈炎）
高安動脈炎
中型血管炎
結節性多発動脈炎（古典的PN）
川崎動脈病
細小血管炎
Wegener肉芽腫症
Churg-Strauss症候群
顕微鏡的多発動脈炎
Schönlein-Henoch紫斑病
原発性クリオグロブリン血症
皮膚白血球破砕性血管炎（過敏性血管炎）

表2　大動脈炎の分類（厚生省調査研究班，1990年）

1. 感染症と関連する大動脈炎
①細菌性大動脈炎（結核性大動脈炎を含む）
②真菌性大動脈炎
③スピロヘータ性大動脈炎ー梅毒性大動脈炎
④その他
2. 膠原病疾患群と関連する大動脈炎
①関節リウマチ
②全身性エリテマトーデス
③リウマチ熱
④再発性多発軟骨炎
⑤その他
3. 血清反応陰性脊椎炎と関連する大動脈炎
①強直性脊椎炎
②Reiter症候群
③その他
4. 原因不明の大動脈炎
①高安大動脈炎
②巨細胞性動脈炎（側頭動脈炎を含む）
③Behçet症候群
④川崎病
⑤いわゆる“inflammatory aneurysm”
⑥非特異性大動脈炎
⑦その他

表3　血管炎症候群の疫学像（文献3より改変引用）

疾患名	推計患者数（95%CI）	男女比	年齢分布	調査年度
結節性多発動脈炎	1,400（1,200～1,700）	1：1.1	56.2（平均）	1994
Wegener肉芽腫症	670（570～780）	1：1.2	46.2（平均）	1994
アレルギー性肉芽腫性血管炎	450（370～530）	1：1.1	47.1（平均）	1994
ANCA関連血管炎	2,700（1,900～2,600）	1：1.8	59.0（平均）	1998
Buerger病	10,000（8,400～12,000）	9.7：1	45～65	1994
高安動脈炎	5,000	1：10	35～65	1993
側頭動脈炎	690（400～980）	1：1.6	62.5（平均）	1998
悪性関節リウマチ	4,200（3,200～5,200）	1：2.2	53.0（平均）	1994
抗リン脂質抗体症候群	3,700（3,300～4,000）	1：6.4	40.8（平均）	1998

経，腎などが多い。

主な血管炎症候群の特徴

(1) PN

KussmaulとMaier (1866年) により報告された疾患 (結節性動脈周囲炎) で，古典的PNともよばれる。病因は不明であるが，HB (hepatitis B) 肝炎ウイルス保持，重篤な中耳炎，薬物過敏症 (メタンフェタミン，サルファ薬，ペニシリンなど) などが誘因または先行する病態としてみられることがある。Cogan症候群はPNの亜型であるが，若年男性に好発し，非梅毒性角膜炎と前庭聴覚障害による症状が先行ないし合併する。

原因不明の発熱，体重減少，関節痛，陰嚢痛などの全身症状をみる。小動脈瘤による皮下結節，網状青色皮斑，結節性紅斑，皮膚潰瘍，指趾壊死，紫斑などの皮膚症状をみるが，皮膚のみに限局した皮膚型PNも存在する。内臓病変では，心筋梗塞，心外膜炎，腎血管病変に伴う腎症，高レニン活性を伴う高血圧，消化管や胆嚢などの臓器梗塞，腸間膜動脈炎による急性腹症，器質的脳症候群，小脳失調，痙攣発作，脳神経症状などが認められる。頭痛，視力障害，脳血管障害は進行する高血圧症によるところが大きい。多発性単神経炎により知覚・運動

表4　血管炎症候群の主な臨床像

	中型血管炎	細小型血管炎			大型血管炎	
疾患	PN	AGA	WG	MPA	側頭動脈炎	高安病
主に侵される動脈の太さ	中，小	小	小	小，細，毛細	大	大
好発年齢	(若)中高年	中年	中年	高齢	高齢(55歳以上)	若年
男女差	男≒女	男≒女	男≒女	問わず	男＝女	男＜女
先行する病態		気管支喘息を含むアレルギー体質	上気道病変，鼻出血，副鼻腔炎，鞍鼻など	感染(気道)		
紫斑，丘疹，水泡，結節	＋	＋	＋	＋＋	－	－
青色皮斑，皮膚潰瘍	＋＋	＋＋	＋	＋＋	－	－
皮下結節	＋＋	＋＋	＋	＋	－	－
筋力低下，筋痛	＋＋	＋＋＋	＋	＋＋	リウマチ性多発筋痛	＋
多発性神経炎	＋＋	＋＋＋	＋	＋＋	－	－
肺浸潤，肺異常陰影	＋	＋＋＋	＋＋＋	＋＋＋	－	－
腎症	＋＋＋	＋	＋＋	＋＋＋	－	－
心病変	＋＋	＋＋	＋	＋	＋	＋＋
高血圧	＋＋＋	－	＋	－	＋	＋＋＋
中枢神経症状	＋＋＋	＋	＋	＋	頭痛	＋＋
視力障害	＋	－	＋	－	＋＋＋	＋＋＋
間欠性跛行	＋	－	－	－	＋＋	＋＋
好酸球増多	＋	＋＋＋	＋	＋	－	－
リウマイド因子	±	＋＋	±	＋	－	－
ANCA	－	＋	＋＋＋	＋＋	－	－
血清低補体価	＋ (HB陽性の場合)	±	±	±	－	－

発熱，体重減少，関節痛は各疾患に共通して認められる。CRP，赤沈亢進も各疾患に共通して認められる。

障害をきたす。

検査所見では，赤沈亢進，CRP強陽性，貧血，白血球増多，血小板増多，尿異常所見，高γグロブリン血症などをみる。抗好中球細胞質抗体(ANCA)は通常陰性である。

腎動脈を含む血管造影で，小動脈瘤，血管壁の不整，狭窄を示す断節的陰影，血管閉塞などをみる。また，皮膚，筋，腎，肝，睾丸などの組織生検により壊死性血管炎を認める。

(2) WG

上気道病変(副鼻腔など)から下気道病変(肺)，腎病変へと進行し，組織学的に壊死性肉芽腫性炎，壊死性血管炎をみる原因不明の疾患である。全身型と限局型がある。

PNと同様の全身症状，皮膚症状をみるが，頻度はPNに比べ少ない。上気道症状はWGの目印となり，化膿性・血性の鼻汁，副鼻腔の疼痛をきたす。鼻粘膜は紅斑性・硬結性潰瘍をきたし，鼻中隔穿孔，鞍鼻をきたす。副鼻腔炎，眼球突出(片側が多い)，結膜炎，上強膜炎，慢性中耳炎，迷路炎，めまい，耳痛，難聴などもみられる。下気道症状では，二次感染を伴っている以外は肺症状に乏しいが，X線上，直径1～9cmの結節性陰影をみる。60～80%に腎症をみるが，早期には尿所見や腎機能障害が軽微であるため見過ごされやすい。

検査所見では，赤沈亢進，CRP強陽性，白血球増多，尿異常所見，腎機能障害などをみる。プロテナーゼ3(proteinase 3；PR3)に対するANCAは本疾患に特異的で90%以上に陽性をみる。生検による病理組織学的所見では，上・下気道病変部の壊死性血管炎と壊死性肉芽腫が特徴的である。細胞浸潤は単球が主体で，巨細胞の出現をみる。

(3) AGA

気管支喘息やアレルギー体質が先行し，好酸球増加とともに血管炎症候をみる。原因は不明であるが，吸引性アレルゲン(阪神淡路大震災後に多発例が報告)やマクロライド系抗生物質，ロイコトリエン受容体拮抗薬などが発症と関連することがある。発熱，体重減少，関節痛，筋肉痛などの全身症状もみられる。肺浸潤は，一過性，移動性としてみられ，非空洞性結節性浸潤やびまん性間質性肺炎はまれである。多発性単神経炎を高率に認め(67%)，知覚障害，運動障害いずれもみられる。

検査所見では，赤沈亢進，白血球増多，高γグロブリン血症に加えて，好酸球の著しい増加が特徴的である。IgEの高値をみることもある。リウマトイド因子を70%に，ミエロペルオキシダーゼに対するANCAを50～80%に認める。

(4) 側頭動脈炎

中・大動脈炎を主徴とする原因不明の疾患である。その病変部位は，頸動脈とその分枝，特に側頭動脈の病変が主であるが，大動脈とその分枝部の病変は10～15%にみられる。臨床症状

はリウマチ性多発筋痛症の症状を伴う。55歳以上の高齢者に発症し，若年者にみられる高安動脈炎と対照的である。側頭動脈炎はリンパ球，マクロファージが巨細胞とともに集積しているのが認められる。そのため，一名巨細胞性動脈炎ともよばれる。内膜は著明に増殖し，内弾性板の断裂を認める。

発熱，体重減少，倦怠感などの全身症状とともに，頭痛，頸部および肩甲部の疼痛と硬直［PMR（polymyalgia

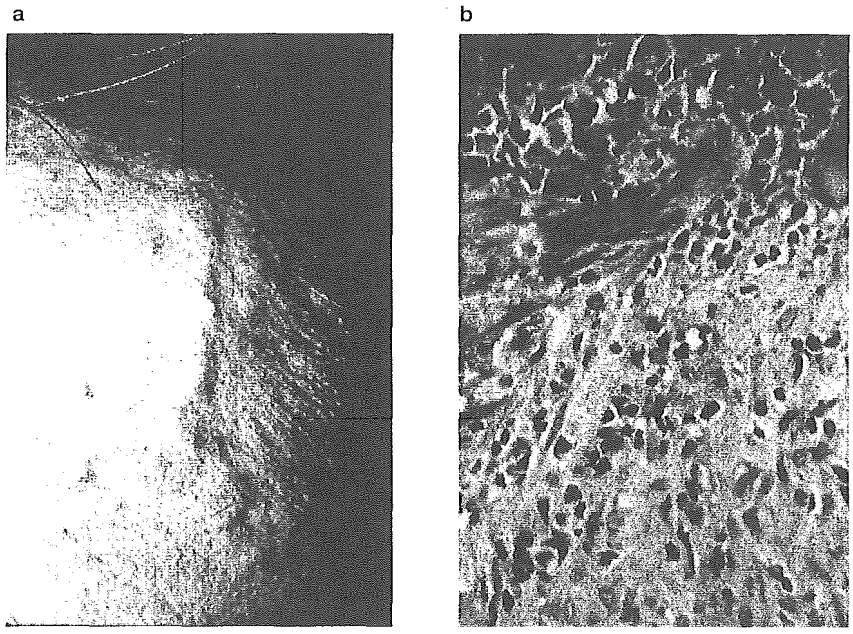

図1　側頭動脈炎
a：側頭動脈の隆起性病変をみる。
b：生検にて動脈壁に巨細胞を伴う血管炎をみる。

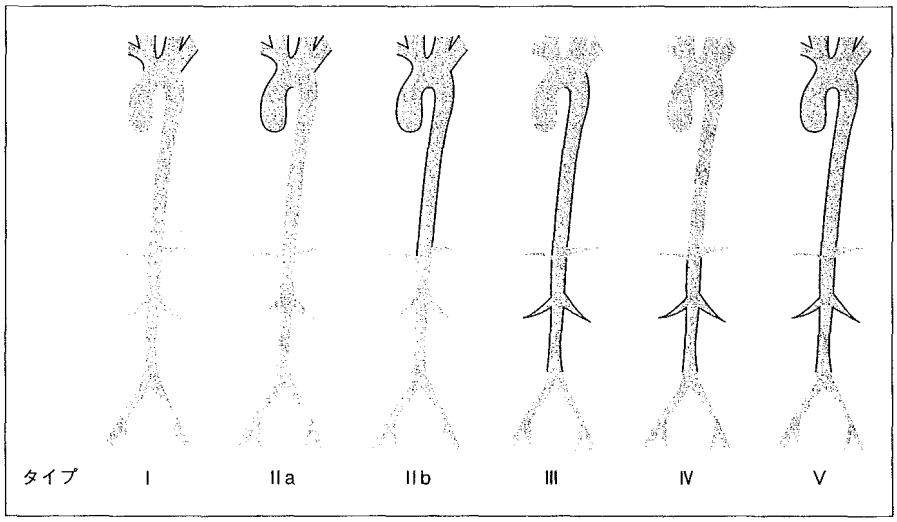

図2　高安動脈炎の病変部位による病型分類
I型：大動脈弓分枝の病変を有するもの。
IIa型：上行大動脈，大動脈弓ならびにその分枝血管に病変を有するもの。
IIb型：上行大動脈，大動脈弓ならびにその分枝血管，胸部下行大動脈に病変を有するもの。
III型：胸部下行大動脈，腹部大動脈，腎動脈に病変を有するもの。
IV型：腹部大動脈ならびに（または）腎動脈に病変を有するもの。
V型：上行大動脈，大動脈弓ならびにその分枝血管，胸部下行大動脈に加え，腹部大動脈ならびに（または）腎動脈病変を有するもの。
日本における病変部位の出現頻度はI型24％，IIa型11％，IIb型10％，III型0％，IV型1％，V型54％でV型が最も多い。

rheumatica) 症状]，間欠性の下顎痛，視力障害などを認める。頭痛は拍動性で，片側性のことが多く，夜間に悪化しやすい。有痛性または肥厚性の側頭動脈を触れる（図1a）。視力障害は50％以上に認められ，10％に失明をみる。眼症状を伴う場合にはPMR症状は少ない。大動脈の障害により間欠性跛行，鎖骨下動脈盗血流症候群，解離性大動脈瘤などをみることがあるが，高安動脈炎に比べ頻度は低い。この他，うつ病，不安感，記銘力低下，器質的脳症状，聴力障害などをみることがある。

検査所見で唯一の異常所見は赤沈亢進である。1時間値80～100mmを示す。自己抗体は通常陰性で，血清筋原性酵素も正常で，筋電図，筋生検も異常を認めない。眼底検査では，視神経乳頭の虚血性変化，網膜の綿花様白斑，小出血などがみられる。側頭動脈生検により巨細胞性動脈炎をみる（図1b）。

(5) 高安動脈炎

原因は不明であるが，大動脈およびその分枝の大・中動脈炎を主徴とする疾患で，別名，脈なし病，大動脈炎症候群ともよばれる。HLA-A24，B52，DR2のハプロタイプとの相関をみる。動脈の炎症は全層にわたり，初期には中・外膜にリンパ球と形質細胞などの細胞浸潤を認め，次いで中膜のびまん性壊死と肉芽腫性反応をきたし，弾力層と平滑筋の破壊をもたらす。壊死巣の周囲には巨細胞，組織球がみられ，治癒期には線維性を示す。弾力層の破壊は動脈瘤形成の要因となる。

発熱，倦怠感，関節痛，筋肉痛などの全身症状をみる。加えて侵される動脈の病変部位により多彩な症状をみる。めまい，頭痛，失神発作，知覚障害，視力障害，間欠性跛行，高血圧などがよくみられる。理学所見では，脈が触れにくい，脈拍の消失・減弱，血圧の左右差，血管雑音などの所見を認める。

検査では，赤沈亢進，CRP陽性，白血球増多，凝固能亢進，高γグロブリン血症，血漿レニン活性高値などをみる。リウマトイド因子や抗核抗体をみることがある。動脈造影所見は重要で，大・中動脈の狭窄，閉塞，拡張，動脈瘤を認める。造影所見により5型に分類される（図2）。眼底所見では乳頭周囲の花環状動静脈吻合が特徴的であるが，高血圧に伴う所見が多い。

文献

1) Jennette JC, Falk RJ, Abdrassy K, et al: Nomenclature of systemic vasculitides, Proposal of an International Consensus Conference. Arthritis Rheum 37: 187-192, 1994.
2) 橋本博史：血管炎症候群.『免疫・アレルギー・リウマチ病学(第2版)』(柏崎禎夫，狩野庄吾，編)，医学書院，東京，1995，p179-208.
3) 難治性血管炎の診療マニュアル．厚生科学研究特定疾患対策研究事業，難治性血管炎に関する調査研究班（班長 橋本博史），2002.
4) Hata A, Noda M, Morowaki R, et al: Angiographic findings of Takayasu arteritis: New classification. Int J Cardiol 54: S155-163, 1996.

The effect of hydrodynamics-based delivery of an IL-13-Ig fusion gene for experimental autoimmune myocarditis in rats and its possible mechanism

Raafat Elnaggar[1], Haruo Hanawa[1], Hui Liu[1], Tsuyoshi Yoshida[1], Manabu Hayashi[1], Ritsuo Watanabe[1], Satoru Abe[1], Ken Toba[1], Kaori Yoshida[1], He Chang[1], Shiro Minagawa[1], Yuji Okura[1], Kiminori Kato[1], Makoto Kodama[1], Hiroki Maruyama[2], Junichi Miyazaki[3] and Yoshifusa Aizawa[1]

[1] Division of Cardiology, Niigata University Graduate School of Medical and Dental Sciences, Niigata, Japan
[2] Division of Clinical Nephrology and Rheumatology, Niigata University Graduate School of Medical and Dental Sciences, Niigata, Japan
[3] Division of Stem Cell Regulation Research, G6, Osaka University Medical School, Suita, Japan

Interleukin (IL)-13 is a pleiotropic cytokine secreted by activated Th2 T lymphocytes. Th1 cytokines are assumed to exacerbate and Th2 cytokines to ameliorate rat experimental autoimmune myocarditis (EAM). Here, we examined the effect of IL-13 on EAM, using a hydrodynamics-based delivery of an IL-13-Ig fusion gene, as well as the possible mechanism of its effect. Rats were immunized on day 0, and IL-13-Ig-treated rats were injected with pCAGGS-IL-13-Ig, and control rats with pCAGGS-Ig, on day 1 or 7. On day 17, the IL-13-Ig gene therapy was effective in controlling EAM as monitored by a decreased heart weight/body weight ratio, by reduced myocarditis and by reduced atrial natriuretic peptide mRNA in the heart, as a heart failure marker. On the basis of IL-13 receptor mRNA expression in separated cells from EAM hearts, we proposed that IL-13-Ig target cells were $CD11b^+$ cells and non-cardiomyocytic noninflammatory (NCNI) cells, such as fibroblasts, smooth muscle or endothelial cells. IL-13-Ig inhibited expression of the genes for prostaglandin E synthase, cyclooxygenase-2, inducible nitric oxide synthase, IL-1β and TNF-α in cultivated cells from EAM hearts, while it enhanced expression of the IL-1 receptor antagonist gene. We conclude that IL-13-Ig ameliorates EAM and suppose that its effectiveness may be due to the influence on these immunologic molecules in $CD11b^+$ and NCNI cells.

Received 19/10/04
Revised 14/3/05
Accepted 12/4/05

[DOI 10.1002/eji.200425776]

Key words: Myocarditis · Autoimmune · Dilated cardiomyopathy · Immune system · IL-13 · Gene therapy

Correspondence: Haruo Hanawa, Division of Cardiology Niigata University Graduate School of Medical and Dental Sciences, 1–757 Asahimachi-dori, Niigata 951–8120, Japan
Fax: +81-25-227-0774
e-mail: hanawara@med.niigata-u.ac.jp

Abbreviations: ANP: Atial natriuretic peptide · **Cox:** Cyclooxygenase · **γc:** Common γ chain · **EAM:** Experimental autoimmune myocarditis · **Glu:** Glucagon · **IL-1RA:** IL-1 receptor antagonist · **iNOS:** Inducible nitric oxide synthase · **NC:** Non-cardiomyocytic · **NCNI:** Non-cardiomyocytic noninflammatory · **PGE2:** Prostaglandin E2 · **PGES:** Prostaglandin E synthase · **SP:** Signal peptide

Introduction

Rat experimental autoimmune myocarditis (EAM) resembles giant cell myocarditis seen in humans [1]. EAM has been shown to be a T cell-mediated autoimmune myocarditis [2], and Th1 and Th2 cytokine balance is thought to be important for controlling progression and repair in EAM. Th1 and Th2 cytokines are produced at different stages of EAM [3]. mRNA for the Th1 cytokines IL-2 and IFN-γ are expressed in the acute phase of EAM in the heart, with the Th2 cytokine

IL-10 increasing later. Some studies have suggested that IL-10 may be effective for the treatment of autoimmune diseases [4, 5], and we also reported that gene transfer of IL-10 into muscle by electroporation *in vivo* was effective for the treatment of EAM [6].

IL-13, secreted by activated Th2 T cells, is a pleiotropic cytokine that regulates a variety of immune target cells. The human IL-13 gene is closely linked to the IL-4 gene on chromosome 5q23–31. They are frequently co-expressed [7] and require the same receptor subunit, IL-4Rα, for signal transduction [8]. Cells that express only the IL-4R, such as human T cells, respond to IL-4 but not to IL-13 [9]. Other cells that do not express the common γ chain (γc), such as X-SCID B cells, fibroblasts and probably endothelial cells, respond to both IL-4 and IL-13 [10]. IL-13 inhibits inflammatory cytokine production by lipopolysaccharide-activated monocytes [11] and prostaglandin E2 (PGE2) production by synovial fibroblasts [12], but induces IgG_4 and IgE synthesis by human B cells [13].

Gene therapy by intra-articular injections of an adenovirus producing rat IL-13 significantly ameliorates the course of rat adjuvant-induced arthritis [14]. However, IL-13 gene therapy has been investigated in only a few other autoimmune diseases, and the use of a naked DNA plasmid in none. Hydrodynamics-based transfection [15] is useful for the delivery of a therapeutic protein into normal rats [16] and into those with glomerulonephritis [17]. Furthermore, fusions of cytokines with Ig-Fc segments secreted as homodimers offer advantages over native cytokines, such as an extended half-life in the circulation, a characteristic of Ig, as well as a higher avidity for the ligand [18]. Here, we tested the effectiveness of IL-13-Ig gene transfer by hydrodynamics-based transfection for the suppression of EAM in rats and investigated the possible mechanism of its effect.

Results

Plasma IL-13-Ig-glucagon-tag protein levels

Plasma IL-13-Ig-glucagon (Glu)-tag protein levels, calculated by using the Glu-tag in rats injected with pCAGGS-IL-13-Ig on day 1, increased, peaking at 48.7±14.8 nmol/l (mean ± SEM) on day 2, and gradually decreased on days 7, 12, and 17 to 7.21±1.91 nmol/l, 0.55±0.13 nmol/l, and 0.21±0.03 nmol/l, respectively. On the other hand, the plasma Ig-Glu-tag protein levels calculated by using the Glu-tag in the pCAGGS-signal peptide (SP)-Ig control rats increased, peaking at 43.4±13.5 nmol/l on day 2, and decreased on days 7, 12, and 17 to 15.0±3.7 nmol/l, 14.2±4.85 nmol/l, and 7.59±1.98 nmol/l, respectively (Fig. 1A) [19]. Plasma IL-13-Ig-Glu-tag protein levels calculated by using the Glu-tag in rats injected with pCAGGS-IL-13-Ig on day 7 increased, peaking at 64.0±7.9 nmol/l (mean ± SEM) on day 8, and gradually decreased on days 11, 14, and 17 to 2.76±0.29 nmol/l, 0.76±0.14 nmol/l, and 0.25±0.04 nmol/l, respectively. These levels were similar to the levels calculated by using IL-13 ELISA (Fig. 1B). It has been reported that IL-13 (5–10 ng/ml, 0.4–0.8 nmol/l) suppresses the production of NO from macrophages *in vitro* [20]. These results indicated that a continuous effective delivery of IL-13-Ig-Glu-tag protein for more than 12 days can be achieved in rats by hydrodynamics-based transfection.

Effect of pCAGGS-rat IL-13-Ig transfer on EAM

IL-13-Ig group rats injected on day 1 (IL-13-Ig group, $n=10$; SP-Ig group, $n=10$) or on day 7 (IL-13-Ig group, $n=7$; SP-Ig group, $n=7$) were more active and had better appetites than SP-Ig group rats. The heart weight/body weight ratio of the IL-13-Ig group was significantly less than that of the SP-Ig group (injection on day 1, 0.45±0.07% versus 0.64±0.09%, $p<0.0001$; injection on day 7, 0.43±0.14% versus 0.79±0.20%, $p=0.0019$) (mean ± SD) (Fig. 2A, D). Many inflammatory cells and fibroblasts had infiltrated into SP-Ig group hearts, but only a few inflammatory cells were found in the hearts of

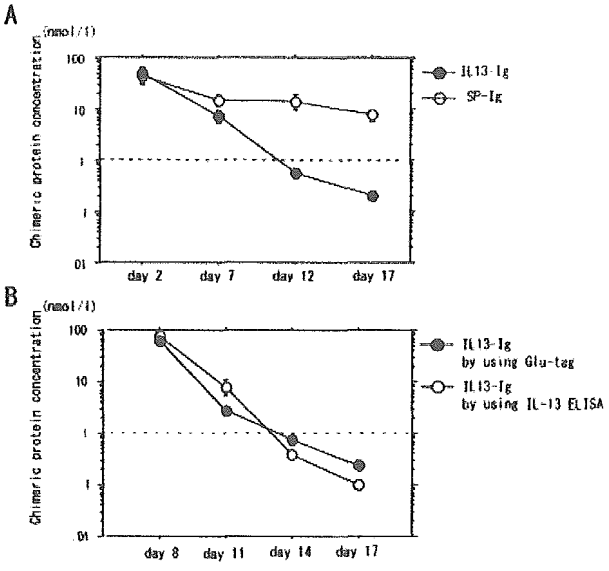

Fig. 1. (A) Plasma Ig-Glu-tag protein (SP-Ig) and IL-13-Ig-Glu-tag protein (IL13-Ig) levels. Rats were injected with pCAGGS-rat SP-Ig-Glu-tag or pCAGGS-rat IL-13-Ig-Glu-tag on day 1. Chimeric protein concentrations were calculated by using Glu-tag. (B) IL-13-Ig-Glu-tag protein (IL13-Ig) levels calculated by using Glu-tag (filled circles) or IL-13 ELISA (empty circles). Rats were injected with pCAGGS-rat IL-13-Ig-Glu-tag on day 7. Error bars represent SEM.

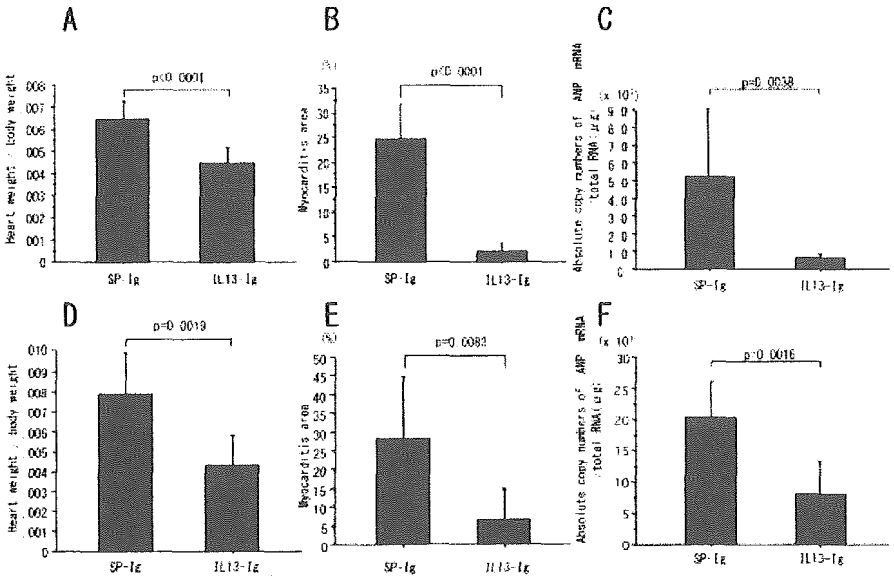

Fig. 2. (A, D) Heart weight/body weight ratio. (B, E) Myocarditis area in EAM hearts. The area was calculated by a color image analyzer using Azan-Mallory-stained specimens. (C, F) Absolute copy numbers of ANP mRNA as a heart failure marker in EAM hearts. (A–C) Rats were injected with plasmid on day 1. (D–F) Rats were injected with plasmid on day 7. Rats were injected with pCAGGS-rat SP-Ig-Glu-tag (SP-Ig) or pCAGGS-rat IL-13-Ig-Glu-tag (IL-13-Ig). Error bars represent SD. Statistical assessment was performed by a non-paired Student's t-test.

the IL-13-Ig-treated group (Fig. 3). The inflammatory area of the ventricle transverse section in the IL-13-Ig group was significantly smaller than in the controls (injection on day 1, 1.94±1.73% versus 25.1±7.3%, $p<0.0001$; injection on day 7, 7.00±8.00% versus 28.5±16.2%, $p=0.0083$) (Fig. 2B, E). Gene expression of atrial natriuretic peptide (ANP) in the heart as a heart failure marker in IL-13-Ig group rats was significantly lower than in SP-Ig group rats (injection on day 1, $6.03\pm3.31\times10^6$ versus $51.4\pm39.9\times10^6$ copies/μg total RNA, $p=0.0038$; injection on day 7, $8.20\pm5.11\times10^7$ versus $20.5\pm5.48\times10^7$ copies/μg total RNA, $p=0.0016$) (Fig. 2C, F). The differences in ANP mRNA levels between rats injected on day 1 and rats injected on day 7 were thought to be due to more severe heart failure of rats injected with a large volume of ringer's solution on day 7 than of those injected on day 1.

Effect of pCAGGS-IL-13-Ig transfer on accumulation of infiltrating cells

In the analysis of infiltrating cells in EAM hearts (Fig. 4), total cells, consisting of $ED1^+$, $CD4^+$ and $CD8^+$ cells in the heart sections, were significantly fewer in the IL-13-Ig group ($n=9$) than in the SP-Ig group ($n=9$) (510±104 versus 1,332±149/specimen, $p<0.0003$) (Fig. 4A).

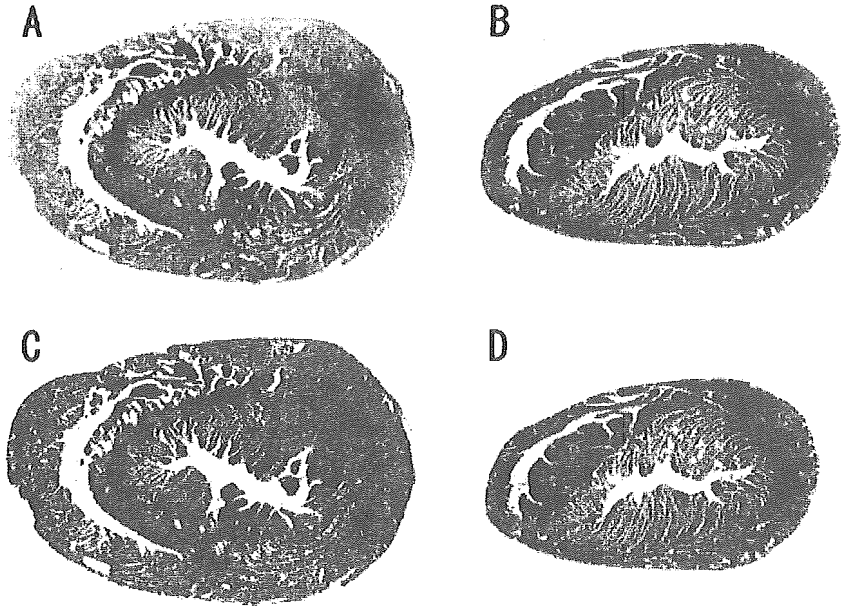

Fig. 3. Histological examination of transverse sections in both ventricles of rats injected on day 1 were stained with Azan-Mallory stain. (A, C) Transverse sections of the hearts in the SP-Ig group; (B, D) transverse sections of the hearts in the IL-13-Ig group. (C, D) Analysis by a color image analyzer. Histological findings of rats injected on day 7 were similar to the above (data not shown).

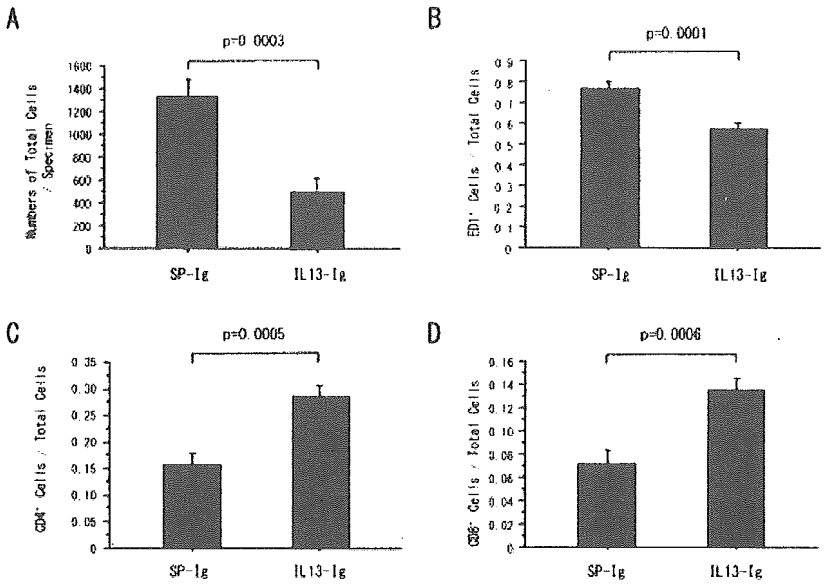

Fig. 4. Infiltrating cells analyzed by immunohistochemistry in EAM hearts from the SP-Ig group (n=9) and the IL-13-Ig group (n=9). SP-Ig, rats were injected on day 1 with pCAGGS-rat SP-Ig-Glu-tag; IL13-Ig, rats were injected on day 1 with pCAGGS-rat IL-13-Ig-Glu-tag. (A) Total cells consisting of ED1$^+$ cells, CD4$^+$ cells and CD8$^+$ cells per specimen of transverse heart sections. (B) ED1$^+$ cells per total cells of transverse heart sections. (C) CD4$^+$ cells per total cells of transverse heart sections. (D) CD8$^+$ cells per total cells of transverse heart sections. Error bars represent SEM. Statistical assessment was performed by a non-paired Student's t-test.

ED1$^+$ cells per total cells were significantly fewer in the IL-13-Ig group than in the SP-Ig group (57.7±2.2% versus 77.1±3.1%, p=0.0001) (Fig. 4B). However, CD4$^+$ cells or CD8$^+$ per total cells were significantly increased in the IL-13-Ig group (CD4$^+$, 28.7±2.0% versus 15.7±2.2%, p=0.0005; CD8$^+$, 13.6±0.9% versus 7.2±1.2%, p=0.0006) (Fig. 4C, D). These results demonstrated that pCAGGS-IL-13-Ig transfer could inhibit the accumulation of macrophages in the inflammatory areas of the heart compared with T cells.

IL-13R and IL-4R mRNA in separated cells from EAM hearts

We separated and purified cardiac myocyte fractions (n=5), αβ T cell fractions (n=5), CD11b$^+$ cell fractions

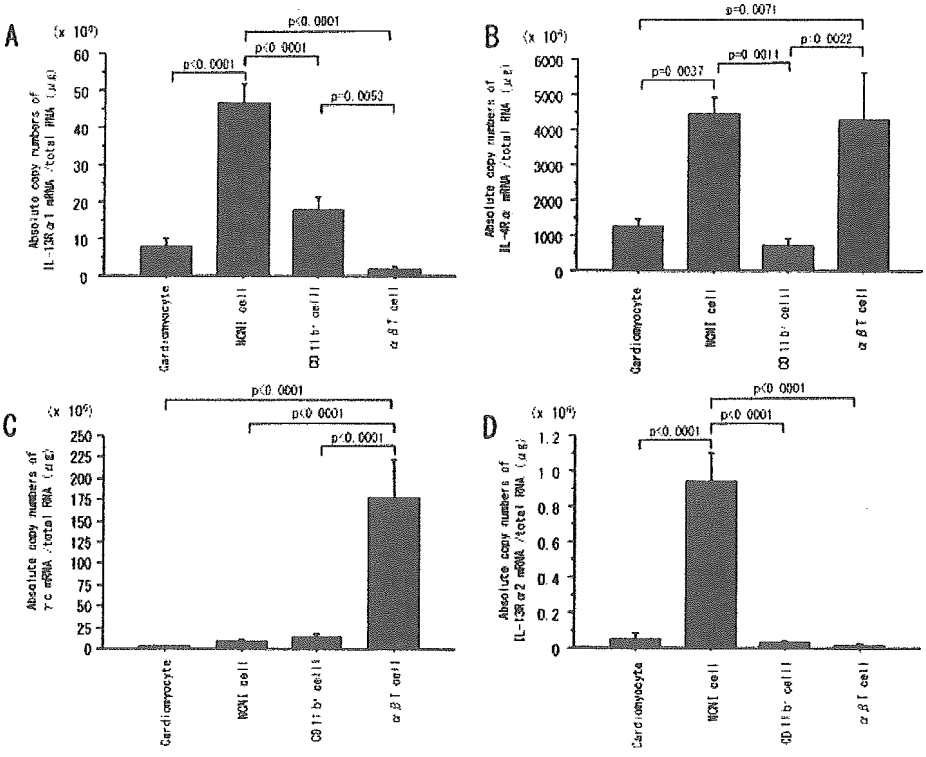

Fig. 5. Absolute copy numbers of IL-13Rα1 (A), IL-4Rα (B), γc (C), and IL-13Rα2 (D) mRNA. Each cell fraction (n=5) was separated and purified from an EAM heart on day 18. NCNI cells contain mainly fibroblasts, smooth muscle cells and endothelial cells. Error bars represent SEM. Statistical assessment was performed by one-way ANOVA and Bonferroni's multiple comparison test. Differences were considered significant at p<0.01. It was suggested that a small number of IL-4Rα mRNA in αβ T cell fractions was due to contamination of CD11b$^+$ cells and NCNI cells. We did not propose that αβ T cells expressed IL-13Rα1 mRNA.

(n=5) and NCNI cell fractions such as fibroblasts, smooth muscle cells or endothelial cells (n=5) from EAM hearts on day 18. NCNI cell fractions and CD11b$^+$ cell fractions clearly expressed IL-13Rα1 mRNA in quantitative real-time PCR analysis (Fig. 5A). However, IL-13Rα1 mRNA levels expressed in αβ T cell fractions were low. This suggested that there was a little contamination of NCNI cells and that αβ T cells did not express IL-13Rα1. The highest level of IL-4Rα, which forms a heterodimer with IL-13Rα1, was detected in the NCNI cell and αβ T cell fractions, but it was detected in all cell fractions. γc, the other molecule which could form a heterodimer with IL-4Rα, was detected in significant amounts in the αβ T cell fractions. IL-13Rα2, which is the decoy receptor for IL-13, was detected in the NCNI cell fractions, but its expression was thought to be considerably weaker than that of IL-13Rα1. IL-13 mRNA in EAM hearts on day 18 was not detected by RT-PCR (data not shown).

mRNA of immunologic molecules in cultivated non-cardiomyocytic cells from EAM hearts

Because we proposed that the target cells for ectopic IL-13-Ig in EAM hearts were CD11b$^+$ (monocytes/macrophages) and NCNI cells (fibroblasts, smooth muscle cells or endothelial cells), we cultivated non-cardiomyocytic (NC) cells, mainly consisting of fibroblasts, CD11b$^+$ cells, smooth muscle cells and endothelial cells, from EAM hearts (Table 1). As genes of prostaglandin E synthase (PGES), cyclooxygenase (Cox)2, inducible nitric oxide synthase (iNOS), IL-1β, TNF-α and IL-1 receptor antagonist (IL-1RA) were expressed mainly by CD11b$^+$ (monocytes/macrophages) or NCNI cells (data not shown), we examined the expression of these genes in cultivated NC cells. IL-13-Ig at a concentration similar to that in serum at the early phase of EAM, significantly inhibited gene expression of PGES, Cox2, iNOS, IL-1β and TNF-α in cultivated NC cells from EAM hearts that were stimulated with IL-1α. IL-13-Ig almost offset the stimulation of cultivated cells by IL-1α in the expression of these genes (Fig. 6). These phenomena were observed with IL-13-Ig at a concentration similar to that in serum at the climax of EAM (Fig. 7). In contrast, IL-13-Ig at a concentration similar to that in serum at the early phase of EAM significantly enhanced the expression of IL-1RA (Fig. 6).

Discussion

Effect of IL-13-Ig gene transfer on EAM

In this study, we demonstrated that pCAGGS-IL-13-Ig gene transfer on day 1 or day 7 by hydrodynamics-based transfection enormously suppressed EAM in rats. It has been reported that gene delivery of recombinant IL-13 or IL-4 by using HSV-1 vectors exerted a protective effect on the development of rat EAE [21, 22]. It is widely reported that Th1 cytokines exacerbate EAE or diabetes in NOD mice, while Th2 cytokines lead to an improvement [4, 5, 21, 22]. In this study, rats in the IL-13-Ig treatment group were very active, with good appetites and only minor myocarditis. This may imply that IL-13-Ig is well tolerated and might be expected to be useful as a drug therapy for certain autoimmune diseases. However, Afanasyeva et al [23] reported that blocking IL-4 with anti-IL-4 mAb reduced the severity of mouse EAM. This issue regarding IL-4, namely a Th2 cytokine acting similarly to IL-13, seems to conflict with our data, and it is difficult to generalize these data rationally. Hesse reported that treatment with an IL-4-neutralizing antibody over a period extending over 6 days post immunization exacerbated the collagen-induced arthri-

Table 1. Absolute copy numbers of specific cell marker mRNA in cultivated NC cells[a)]

	Copy numbers of mRNA/μg of total RNA
	NC cells (n=6)
CD3	19,100±12,100
Collagen type III	228,000,000±91,800,000
Calponin	2,220,000±1,090,000
CD11b	4,330,000±1,670,000
von Willebrand factor	82,300±36,700
α cardiac myosin	N.D.

[a)] Results are expressed as the mean ± SEM. ND: not detected.

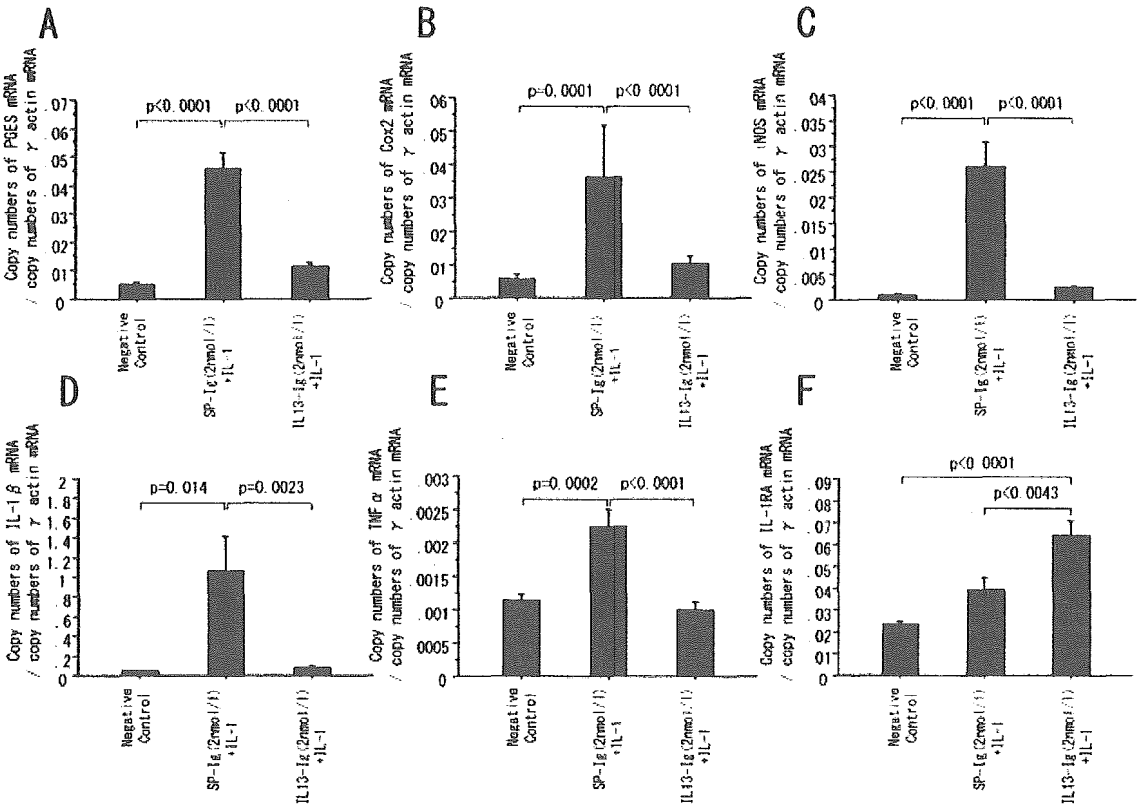

Fig. 6. Copy numbers of mRNA of various immunological molecules per copy number of γ-actin mRNA in cultivated NC cells (n=6) from EAM hearts in uncoated plates. NC cells contain mainly fibroblasts, smooth muscle cells, endothelial cells and CD11b$^+$ cells. (A) PGES, (B) Cox2, (C) iNOS, (D) IL-1β, (E) TNF-α, (F) IL-1RA. Negative control, cells were cultivated in medium containing neither IL-1α nor rat serum; SP-Ig + IL-1, cells were cultivated in medium with IL-1α and serum of a normal rat injected with pCAGGS-SP-Ig-Glu-tag; IL-13-Ig + IL-1, cells were cultivated in medium with IL-1α and serum of a normal rat injected with pCAGGS-IL-13-Ig-Glu-tag. The final concentration of Ig-Glu-tag protein or IL-13-Ig-Glu-tag protein is 2 nmol/l. The concentration of IL-13-Ig-Glu-tag protein is similar to that in serum at the early phase of EAM in rats injected with pCAGGS-IL-13-Ig-Glu-tag on day 1 or day 7. Error bars represent SEM. Statistical assessment was performed by one-way ANOVA and Bonferroni's multiple comparison test. Differences were considered significant at $p<0.01$.

tis, but when curtailed to 2 days post immunization, the disease was reduced [24]. Anti-IL-4 antibody therapy may act in a complicated way in the course of an autoimmune disease. In addition, there may be a difference between rat EAM and mouse EAM or between IL-4 action and IL-13 action for EAM, as mentioned above. Further studies are necessary to clearly explain this issue.

Target cells of IL-13-Ig

IL-13 is thought to act not on αβ T cells but on NCNI cells and CD11b$^+$ cells in EAM hearts, because these cells express both IL-4Rα and IL-13Rα1. As gene transfer of IL-13-Ig on day 7, namely the time just before onset, significantly reduced EAM, we suggest that IL-13-Ig acted on these target cells in EAM hearts. It is generally agreed that IL-13 acts on monocytes and B cells, but not on T cells [25]. On the other hand, IL-4 is thought to act on not only these cells but also on αβ T cells, which have both IL-4Rα and γc. Actually, infiltrating cells suppressed by the pCAGGS-IL-13-Ig gene transfer were mainly ED1$^+$ cells. ED1$^+$ cells are thought to be macrophages, while IL-13R-positive NCNI cells may be fibroblasts, endothelial cells and smooth muscle cells [26]. The target cells on which IL-13 directly acts are generally supposed to be macrophages, fibroblasts, smooth muscle cells, endothelial cells and B cells [27].

Role of IL-13 target cells in EAM

Of the infiltrating mononuclear cells in EAM hearts, 70–80% are macrophages [28], and IL-1, TNF-α and iNOS produced by them play an important role in the pathogenesis of EAM [29]. On the other hand, the role of NCNI cells in EAM has not yet been fully examined. Myocardial fibroblasts in coxsackievirus B3 myocarditis produce pro-inflammatory cytokines [30]. In rheuma-

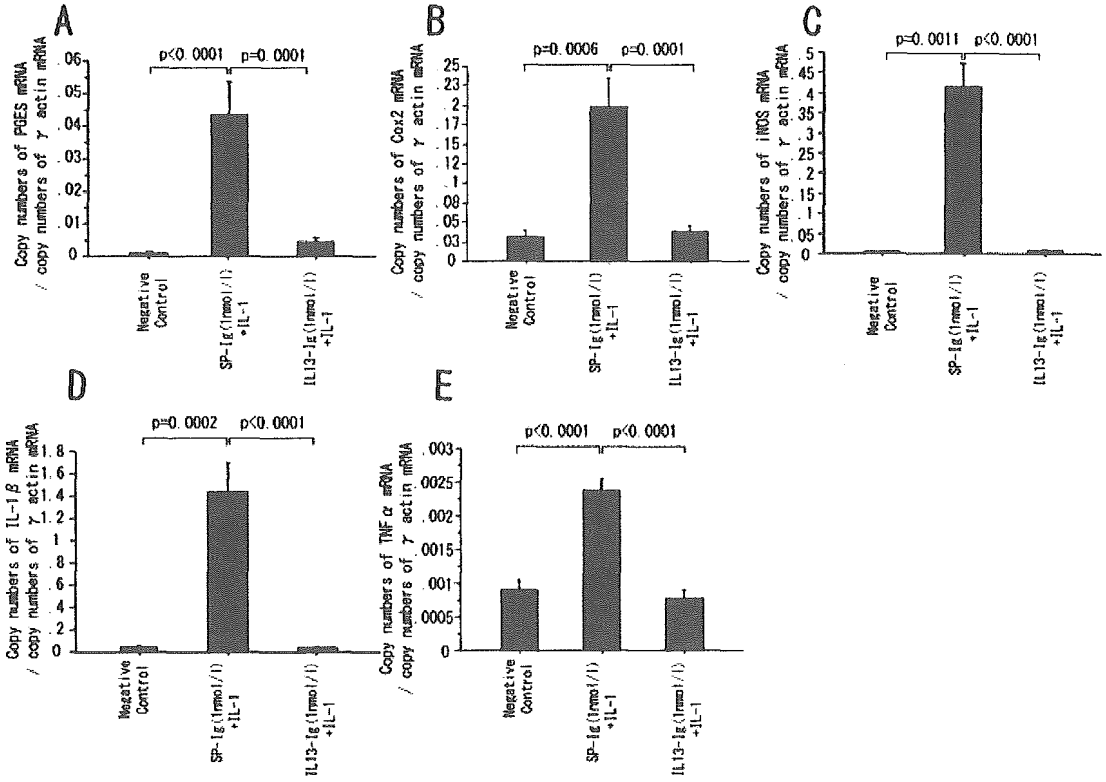

Fig. 7. Copy numbers of mRNA of various immunological molecules per copy number of γ-actin mRNA in cultivated NC cells (n=8) *from EAM hearts in uncoated plates.* (A) PGES, (B) Cox2, (C) iNOS, (D) IL-1β, (E) TNF-α. Negative control, SP-Ig + IL-1 and IL-13-Ig + IL-1 as defined in Fig. 6. Final concentration of Ig-Glu-tag protein or IL-13-Ig-Glu-tag protein is 1 nmol/l. The concentration of IL-13-Ig-Glu-tag protein is similar to that in serum at the climax of EAM in rats injected with pCAGGS-IL-13-Ig-Glu-tag on day 7. Expressions levels of IL-1RA were not significantly different among the groups (data not shown). Error bars represent SEM. Statistical assessment was performed by one-way ANOVA and Bonferroni's multiple comparison test. Differences were considered significant at $p<0.01$.

toid arthritis, fibroblasts were thought to play an important role in cartilage damage [31]. Because EAM is similar to rheumatoid arthritis, fibroblasts in EAM hearts may resemble synovial fibroblast with regard to pathogenesis. More than 90% of the interstitial cells in the heart are fibroblasts before an inflammatory infiltration develops [32]. Fibroblasts are therefore likely to play an active role in the inflammatory reactions. PGE2, produced by Cox2 and PGES, contributes to the pathogenesis of rheumatoid arthritis, acting as a mediator of inflammation and promoting bone destruction [33].

Effect of IL-13-Ig on target cells in EAM

It is well documented that IL-13 inhibits the production of PGES, Cox2, iNOS and cytokines such as IL-1 or TNF-α in fibroblasts or macrophages, but enhances IL-1RA production [12, 20, 27, 34–36]. This study demonstrated that serum containing IL-13-Ig inhibited PGES, Cox2, IL-1β, iNOS and TNF-α gene expression in NC cells (mainly fibroblasts, smooth muscle cells, endothelial cells and $CD11b^+$ cells) in EAM hearts, while it enhanced the expression of IL-1RA. Therefore, the IL-13-Ig was thought to act as an agonist at the IL-13R and suppress EAM. The concentration of IL-13-Ig used in the *in vitro* experiments was similar to that in serum at the acute phase or climax of EAM. IL-13-Ig produced by hydrodynamics-based transfection was thought to influence the $CD11b^+$ cells and NCNI cells *in vivo* as well.

Th1 cytokines play an important role in EAM; however, since we did not propose that αβ T cells producing Th1 cytokines such as IL-2 or IFN-γ expressed the IL-13Rα1 gene, we did not analyze them. IL-13-Ig slightly decreased expression of the IL-12 gene, inducing Th1 cytokines in cultivated NC cells and spleen cells from EAM rats, but the difference was not significant (data not shown). Therefore, this study could not demonstrate that IL-13-Ig had a major influence on the production of Th1 cytokines.

Hydrodynamics-based plasmid DNA delivery for various diseases

Hydrodynamics-based gene delivery can transfer into hepatocytes by retrograde blood flow from hepatic veins. Hydrodynamics-based transfection is more efficient for the production of a therapeutic protein than gene transfer into muscle by electroporation *in vivo*, because the former method allows greater retention of synthesized proteins in the plasma than the latter [6]. Because gene transfer by a plasmid vector is easier and safer than by a virus vector, it is likely that hydrodynamics-based transfection by plasmid DNA will find more applications in the future for the analysis of protein drug effects on various diseases. On the other hand, Maruyama et al. [37] reported high levels of gene expression in kidney cells through a hydrodynamic infusion of DNA solution into the renal vein. Therefore, if a modified hydrodynamics-based transfection into the heart, such as retrograde coronary venous delivery [38], is established, it may be useful for therapy in human myocarditis.

Materials and methods

Animals

Lewis rats were obtained from Charles River, Japan (Atsugi, Kanagawa, Japan), and were maintained in our animal facilities until they reached 8 weeks of age. Throughout the studies, all the animals were treated in accordance with the guidelines for animal experiments of our institute.

Plasmid DNA for gene transfer

To create plasmids for the experiment, we first constructed the plasmid pCAGGS-Ig-Glu-tag [19] with Swa I and Not I restriction sites using PCR. The first PCR products were amplified from rat spleen cDNA using KOD Plus DNA polymerase (TOYOBO, Osaka, Japan) and the primers 5′-gaGAATTCATTTAAATgagaGCGGCCGCgtgcccagaaactgtg-3′ (with Swa I and Not I restriction sites) and 5′-tcaaccactgcacaaaatcttgggctttacccggagagtgggagagact-3′. The final PCR product inserts were then amplified from the diluted products of the first PCR reaction with the primers 5′-gaGAATTCATTTAAATgagaGCGGCCGCgtgcccagaaactgtg-3′ (with Swa I and Not I restriction sites) and 5′-gagagagaGAATTCtcaggtattcatcaaccactgcacaaaatcttgggc-3′. These products were inserted into the pCAGGS vector using EcoR I sites. *Escherichia coli* JM109 competent cells were then transformed, and recombinant plasmids were isolated using a Quantum Prep Plasmid Maxiprep kit (Bio-Rad Laboratories, Hercules, CA). In addition, when constructing the control plasmid, pCAGGS-SP-Ig-Glu-tag, SP of secretory leukocyte protease inhibitor cDNA was amplified from EAM heart cDNA using the primers 5′-gaGAATTCATTTAAATgaagtccagcggcctcttcccc-3′ and 5′-gcagcatcGCGGCCGCtccttccacactccagggtgccag-3′ and then inserted into pCAGGS-Ig-Glu-tag using the Swa I and Not I sites. To construct pCAGGS-rat IL-13-Ig-Glu-tag, rat IL-13 cDNA was amplified from phytohemagglutinin-stimulated splenocyte cDNA using the primers 5′-gaGAATTCATTTAAATggcactctgggtgactgcagtc-3′ and 5′-gcagcatcGCGGCCGCgtggccatagcggaaaagttgctt-3′ and then inserted into pCAGGS-Ig-Glu-tag using the Swa I and Not I sites. The recombinant plasmids were isolated as described above.

Induction of EAM

Whole cardiac myosin was prepared from the ventricular muscle of porcine hearts as described [39]. It was dissolved in a solution of 0.3 mol/l KCl at a concentration of 10 mg/ml and emulsified with an equal volume of complete Freund's adjuvant supplemented with 10 mg/ml *Mycobacterium tuberculosis* H37RA (Difco, Detroit, Michigan). On day 0, the rats received a single immunization at two subcutaneous sites on the foot with a total of 0.2 ml emulsion for each rat.

Plasmid DNA injection

Rats (34) were divided into four groups (injection on day 1: IL-13-Ig group, $n=10$; SP-Ig group, $n=10$; injection on day 7: IL-13-Ig group, $n=7$; SP-Ig group, $n=7$) and were injected with 800 μg pCAGGS-rat IL-13-Ig-Glu-tag or pCAGGS-SP-Ig-Glu-tag that was mixed with an appropriate volume of ringer's solution (approximately 80 ml/kg body weight) via the tail vein within 15 s on day 1 or day 7 [16]. Because EAM occurs from day 9 or day 10, injection of a large volume after day 8 for gene transfer is thought to cause death due to heart failure. Therefore, we transferred the IL-13-Ig gene on day 7 to examine the direct effects in hearts without the effects in lymphoid organs.

Plasma chimeric Glu-tag protein measurement

Blood samples were taken on days 2, 7, 12, and 17 after gene transfer on day 1, and on days 8, 11, 14, and 17 after gene transfer on day 7. Glu concentrations were measured using a Glu RIA Kit (DAIICHI RADIOISOTOPE LABS, Tokyo, Japan) [40], and rat IL-13 concentration was measured using a rat IL-13 ELISA kit (Biosource International, Camarillo, CA). Chimeric protein concentrations were calculated using Glu-tag [(chimeric protein concentration) (nmol/l) = (actually measured Glu concentration) (ng/l)/(whole Glu molecular weight)] or using rat IL-13 [(chimeric protein concentration) (nmol/l) = (actually measured IL-13 concentration) (ng/l)/(whole IL-13 molecular weight)].

Evaluation of histopathology

Heart weight and body weight were measured, and the ratio of heart weight to body weight (g/g) was calculated. After embedding in paraffin, several transverse sections were cut from the mid-ventricle slice and stained with hematoxylin-eosin and Azan-Mallory. The myocarditis area was determined using the specimen stained with Azan-Mallory by a color image analyzer (Mac SCOPE version 2.6; MITANI Corporation, Japan).

Table 2. List of primers for quantitative RT-PCR

	Sense Primer	Antisense Primer
ANP	5'-atggatttcaagaacctgctagac-3'	5'-gctccaatcctgtcaatcctac-3'
α cardiac myosin	5'-acaaggttaaaaacctgacagagg-3'	5'-tactgttctgctgactgatgtcaa-3'
CD3	5'-gatcccaaactctgctatatgcta-3'	5'-ctttcatgccaatctcactgtag-3'
CD11b	5'-gggatccgtaaagtagtgagaa-3'	5'-aaaggagctggtacttcctgtct-3'
collagen type III	5'-cgcaattgcagagacctgaa-3'	5'-acagtcatgggactggcatttat-3'
von Willebrand factor	5'-agaggctacacatctctcagaagc-3'	5'-gaccttcttcttcttgaaaccttg-3'
calponin	5'-aacataggaaatttcatcaaagcc-3'	5'-gtagactgatagttgcctgatcca-3'
IL-13Rα1	5'-gaagcgctgagtataggtaaggag-3'	5'-ccgctttctttaggttttctatca-3'
IL-13Rα2	5'-ctatgtttttctggtatgagggct-3'	5'-aatatcatcttctcggaccacaat-3'
IL-4Rα	5'-taccggagttttagtgacttctcc-3'	5'-gagaaagccttgtaaccagtgtct-3'
γc chain	5'-tgccatctagatccttcttactcc-3'	5'-tcttttgagaacagatagtggctg-3'
PGES	5'-gtgatggagaacagccagg-3'	5'-gaggaccacgaggaaatgtatc-3'
Cox2	5'-tgtgatattctcaaacaggagcat-3'	5'-aaggaggatggagttgttgtagag-3'
iNOS	5'-ttctactattaccagatcgagccc-3'	5'-gtagttgttcctcttccaaggtgt-3'
IL-1β	5'-gctagtgtgtgatgttcccattag-3'	5'-cttttccatcttcttctttgggta-3'
TNFα	5'-atgggctccctctcatcagt-3'	5'-actccagctgctcctctgct-3'
IL-1RA	5'-agaagaaaagatagacatggtgcc-3'	5'-actttgtgactgtacagggctctt-3'
γ-actin	5'-agccttccttcctgggcatggagt-3'	5'-tggaggggcctgactcgtcatact-3'

Immunohistochemical staining

Hearts harvested on day 17 after the gene transfer on day 1 were embedded in Tissue-Tek OCT compound (Miles Inc. Elkhart, IN) and frozen at –80°C. Transverse sections 6 μm thick were cut from the mid-ventricle slice with a cryostat and fixed in ether for 10 min. The presence of macrophages, $CD4^+$ T cells and $CD8^+$ T cells was examined immunohistochemically using a mouse mAb against rat macrophages (ED1; Serotec, Oxford, UK), a mouse mAb against rat CD4 (W 3/25; Serotec) or CD8 (OX-8; Serotec), biotinylated goat anti-mouse IgG_1 (Amersham, UK) and labeled streptavidin-horseradish peroxidase (Amersham). Specimens in which many infiltrating cells were observed were then selected, and total $ED1^+$, $CD4^+$ and $CD8^+$ cells of the IL-13 group ($n=9$) and the Ig control group ($n=9$) were counted.

RNA extraction from cells separated from EAM hearts

To measure mRNA of ANP as heart failure marker, total RNA was isolated from one third of the apical area of the heart on day 17 (injection on day 1: pCAGGS-IL-13-Ig group, $n=9$; pCAGGS-SP-Ig group, $n=8$; injection on day 7: pCAGGS-IL-13-Ig group, $n=7$; pCAGGS-SP-Ig group, $n=7$) using Trizol (Invitrogen, Tokyo, Japan). To evaluate IL-13 target cells expressing IL-13Rα1 mRNA, cardiomyocytes and the other cells in hearts of EAM rats ($n=5$) on day 18 were isolated after collagenase perfusion treatment for 20 min using a Langendorff apparatus, as reported [41]. Briefly, isolated cells in an isotonic buffer were separated serially through stainless steel sieves into cardiomyocytes and other cells. Because almost all inflammatory cells in EAM hearts are $CD11b^+$ cells and αβ T cells [28], the other cells were separated into αβ T cells, $CD11b^+$ cells and NCNI cells such as fibroblasts, smooth muscle cells or endothelial cells by anti-PE microbeads (Miltenyi Biotec, Bergisch Gladbach, Germany) and a MACS magnetic cell sorting system (Miltenyi Biotech) using appropriate mAb, namely PE-conjugated anti-TCRα/β (R73) and anti-CD11b mAb (OX-42) (PharMingen, San Diego, CA). The fractions of cardiomyocytes, αβ T cells, $CD11b^+$ cells and NCNI cells were confirmed by analysis of specific marker gene expression, namely, α-cardiac myosin, CD3, CD11b, collagen type β, calponin and von Willebrand factor, and even at the highest level of contamination, it was under 10% (data not shown). Total RNA was isolated from each purified cell fraction (cardiomyocytes, $CD11b^+$ cells, αβ T cells and NCNI cells) of EAM hearts on day 18 (acute phase, $n=5$) using Trizol. cDNA was synthesized from 2–5 μg total RNA with random primers and murine Moloney leukemia virus reverse transcriptase in a final volume of 20 μl.

Cell culture

To evaluate the effect of IL-13-Ig on the target cells in EAM hearts, NC cells of EAM rat hearts on day 18 were isolated after digestion with collagenase (40 mg/100 ml) and trypsin (100 mg/100 ml) solution. The cells were cultured in 2 ml RPMI medium supplemented with 10% FCS on uncoated plates. After overnight incubation, the supernatant was rinsed off and the medium was changed every 2 days, and after one week, the cells achieved confluence. IL-1α (60 ng) was added to stimulate these cells, and then serum of a rat injected with pCAGGS-IL-13-Ig-Glu-tag (IL-13-Ig-Glu-tag protein, final concentration 2 nmol/l or 1 nmol/l) or serum of a rat injected with pCAGGS-SP-Ig-Glu-tag (Ig-Glu-tag protein, final concentration 2 nmol/l or 1 nmol/l) was added to these dishes (IL-13-Ig + IL-1α group, SP-Ig + IL-1α group, non-serum and non-IL-1α group). An amount of 2 nmol/l of IL-13-Ig-Glu-tag protein is similar to that in serum at the acute phase of EAM and 1 nmol/l is similar to that in serum at the climax of EAM in rats injected with pCAGGS-IL-13-Ig-Glu-tag on day 7. After 24 h, these cells were harvested and used for quantitative real-time PCR analysis to examine gene expression of PGES, Cox2, iNOS, IL-1β, TNF-α and IL-1RA. These cultivated cells were thought to contain mainly fibroblasts, $CD11b^+$ cells, smooth muscle cells and endothelial cells as determined by gene expression analysis (Table 1).

Quantitative real-time PCR analysis

To create the plasmids used for the standard, cDNA amplified from an EAM heart using the primers indicated in Table 2 was directly inserted into the pGEM-T vector, and the recombinant plasmids were isolated after transforming *Escherichia coli* JM109 competent cells using a MagExtractor plasmid Kit (TOYOBO, Osaka, Japan). cDNA was diluted 100-fold with DNase-free water, then 5 μl was used for real-time PCR. cDNA and diluted plasmid were amplified with the same primers used for making the plasmid and a LightCycler-FastStart DNA Master SYBR Green I kit (Roche, Indianapolis, IN). After an initial denaturation step of 10 min at 95°C, a three-step cycle procedure was used (denaturation at 95°C for 10 s, annealing at 62°C for 10 s, and extension at 72°C for 13 s, for 40 cycles). LightCycler Software calculated the standard curve using five plasmid standards. The absolute copy numbers of all samples were calculated by LightCycler software using this standard curve [3].

Statistical analysis

Statistical assessment was performed by a non-paired Student's *t*-test or one-way ANOVA and Bonferroni's multiple comparison test with StatView 5.0 (SAS Institute Inc.). The differences were considered significant at $p<0.01$. Data obtained from the quantitative RT-PCR for specific cell markers and immunological molecules, immunohistochemistry data and concentrations of Ig-Glu-tag protein and IL-13-Ig-Glu-tag protein are expressed as means ± SEM. Copy numbers of ANP mRNA, heart/body weight ratio and myocarditis area are expressed as means ± SD.

Acknowledgements: This study was supported in part by grants for scientific research from the Ministry of Education, Science, and Culture of Japan (Nos. 12670653, 14570645) and for Research on Specific Diseases of Ministry of Health, Labor and Welfare.

References

1 **Kodama, M., Matsumoto, Y., Fujiwara, M., Zhang, S. S., Hanawa, H., Itoh, E., Tsuda, T., Izumi, T. and Shibata, A.,** Characteristics of giant cells and factors related to the formation of giant cells in myocarditis. *Circ. Res.* 1991. **69:** 1042–1050.

2 **Kodama, M., Matsumoto, Y. and Fujiwara, M.,** *In vivo* lymphocyte-mediated myocardial injuries demonstrated by adoptive transfer of experimental autoimmune myocarditis. *Circulation* 1992. **85:** 1918–1926.

3 **Hanawa, H., Abe, S., Hayashi, M., Yoshida, T., Yoshida, K., Shiono, T., Fuse, K., Ito, M., Tachikawa, H., Kashimura, T. et al.,** Time course of gene expression in rat experimental autoimmune myocarditis. *Clin. Sci.* 2002. **103:** 623–632.

4 **Yang, Z., Chen, M., Wu, R., Fialkow, L. B., Bromberg, J. S., McDuffie, M., Naji, A. and Nadler, J. L.,** Suppression of autoimmune diabetes by viral IL-10 gene transfer. *J. Immunol.* 2002. **168:** 6479–6485.

5 **Goudy, K., Song, S., Wasserfall, C., Zhang, Y. C., Kapturczak, M., Muir, A., Powers, M., Scott-Jorgensen, M., Campbell-Thompson, M., Crawford, J. M. et al.,** Adeno-associated virus vector-mediated IL-10 gene delivery prevents type 1 diabetes in NOD mice. *Proc. Natl. Acad. Sci. USA* 2001. **98:** 13913–13918.

6 **Watanabe, K., Nakazawa, M., Fuse, K., Hanawa, H., Kodama, M., Aizawa, Y., Ohnuki, T., Gejyo, F., Maruyama, H. and Miyazaki, J.,** Protection against autoimmune myocarditis by gene transfer of interleukin-10 by electroporation. *Circulation* 2001. **104:** 1098–1100.

7 **Dolganov, G., Bort, S., Lovett, M., Burr, J., Schubert, L., Short, D., McGurn, M., Gibson, C. and Lewis, D. B.,** Coexpression of the interleukin-13 and interleukin-4 genes correlates with their physical linkage in the cytokine gene cluster on human chromosome 5q23–31. *Blood* 1996. **87:** 3316–3326.

8 **Mueller, T. D., Zhang, J. L., Sebald, W. and Duschl, A.,** Structure, binding, and antagonists in the IL-4/IL-13 receptor system. *Biochim. Biophys. Acta* 2002. **1592:** 237–250.

9 **Zurawski, S. M., Vega, F., Jr., Huyghe, B. and Zurawski, G.,** Receptors for interleukin-13 and interleukin-4 are complex and share a novel component that functions in signal transduction. *EMBO J.* 1993. **12:** 2663–2670.

10 **Callard, R. E., Matthews, D. J. and Hibbert, L.,** IL-4 and IL-13 receptors: are they one and the same? *Immunol. Today* 1996. **17:** 108–110.

11 **de Waal Malefyt, R., Figdor, C. G., Huijbens, R., Mohan-Peterson, S., Bennett, B., Culpepper, J., Dang, W., Zurawski, G. and de Vries, J. E.,** Effects of IL-13 on phenotype, cytokine production, and cytotoxic function of human monocytes. Comparison with IL-4 and modulation by IFN-gamma or IL-10. *J. Immunol.* 1993. **151:** 6370–6381.

12 **Alaaeddine, N., Di Battista, J. A., Pelletier, J. P., Kiansa, K., Cloutier, J. M. and Martel-Pelletier, J.,** Inhibition of tumor necrosis factor alpha-induced prostaglandin E2 production by the antiinflammatory cytokines interleukin-4, interleukin-10, and interleukin-13 in osteoarthritic synovial fibroblasts: distinct targeting in the signaling pathways. *Arthritis Rheum.* 1999. **42:** 710–718.

13 **Punnonen, J., Aversa, G., Cocks, B. G., McKenzie, A. N., Menon, S., Zurawski, G., de Waal Malefyt, R. and de Vries, J. E.,** Interleukin 13 induces interleukin 4-independent IgG4 and IgE synthesis and CD23 expression by human B cells. *Proc. Natl. Acad. Sci. USA* 1993. **90:** 3730–3734.

14 **Woods, J. M., Amin, M. A., Katschke, K. J., Jr., Volin, M. V., Ruth, J. H., Connors, M. A., Woodruff, D. C., Kurata, H., Arai, K., Haines, G. K., 3rd. et al.,** Interleukin-13 gene therapy reduces inflammation, vascularization, and bony destruction in rat adjuvant-induced arthritis. *Hum. Gene Ther.* 2002. **13:** 381–393.

15 **Liu, F., Song, Y. and Liu, D.,** Hydrodynamics-based transfection in animals by systemic administration of plasmid DNA. *Gene Ther.* 1999. **6:** 1258–1266.

16 **Maruyama, H., Higuchi, N., Nishikawa, Y., Kameda, S., Iino, N., Kazama, J. J., Takahashi, N., Sugawa, M., Hanawa, H., Tada, N. et al.,** High-level expression of naked DNA delivered to rat liver via tail vein injection. *J. Gene Med.* 2002. **4:** 333–341.

17 **Higuchi, N., Maruyama, H., Kuroda, T., Kameda, S., Iino, N., Kawachi, H., Nishikawa, Y., Hanawa, H., Tahara, H., Miyazaki, J. et al.,** Hydrodynamics-based delivery of the viral interleukin-10 gene suppresses *experimental crescentic glomerulonephritis in Wistar-Kyoto rats. Gene Ther.* 2003. **10:** 1297–1310.

18 **Jiang, J., Yamato, E. and Miyazaki, J.,** Sustained expression of Fc-fusion cytokine following *in vivo* electroporation and mouse strain differences in expression levels. *J. Biochem. (Tokyo)* 2003. **133:** 423–427.

19 **Hanawa, H., Watanabe, R., Hayashi, M., Yoshida, T., Abe, S., Komura, S., Liu, H., Elnaggar, R., Chang, H., Okura, Y. et al.,** A novel method to assay proteins in blood plasma after intravenous injection of plasmid DNA. *Tohoku J. Exp. Med.* 2004. **202:** 155–161.

20 **Bogdan, C., Thuring, H., Dlaska, M., Rollinghoff, M. and Weiss, G.,** Mechanism of suppression of macrophage nitric oxide release by IL-13: influence of the macrophage population. *J. Immunol.* 1997. **159:** 4506–4513.

21 **Cash, E., Minty, A., Ferrara, P., Caput, D., Fradelizi, D. and Rott, O.,** Macrophage-inactivating IL-13 suppresses experimental autoimmune encephalomyelitis in rats. *J. Immunol.* 1994. **153:** 4258–4267.

22 **Furlan, R., Poliani, P. L., Marconi, P. C., Bergami, A., Ruffini, F., Adorini, L., Glorioso, J. C., Comi, G. and Martino, G.,** Central nervous system gene therapy with interleukin-4 inhibits progression of ongoing relapsing-remitting autoimmune encephalomyelitis in Biozzi AB/H mice. *Gene Ther.* 2001. **8:** 13–19.

23 **Afanasyeva, M., Wang, Y., Kaya, Z., Park, S., Zilliox, M. J., Schofield, B. H., Hill, S. L. and Rose, N. R.,** Experimental autoimmune myocarditis in A/J mice is an interleukin-4-dependent disease with a Th2 phenotype. *Am. J. Pathol.* 2001. **159:** 193–203.

24 **Hesse, M., Bayrak, S. and Mitchison, A.,** Protective major histocompatibility complex genes and the role of interleukin-4 in collagen-induced arthritis. *Eur. J. Immunol.* 1996. **26:** 3234–3237.

25 **Zurawski, G. and de Vries, J. E.,** Interleukin 13, an interleukin 4-like cytokine that acts on monocytes and B cells, but not on T cells. *Immunol. Today* 1994. **15:** 19–26.

26 **Doucet, C., Brouty-Boye, D., Pottin-Clemenceau, C., Jasmin, C., Canonica, G. W. and Azzarone, B.,** IL-4 and IL-13 specifically increase *adhesion molecule and inflammatory cytokine expression in human lung* fibroblasts. *Int. Immunol.* 1998. **10:** 1421–1433.

27 **Wynn, T. A.,** IL-13 effector functions. *Annu. Rev. Immunol.* 2003. **21:** 425–456.

28 **Kodama, M., Zhang, S., Hanawa, H. and Shibata, A.,** Immunohistochemical characterization of infiltrating mononuclear cells in the rat heart with experimental autoimmune giant cell myocarditis. *Clin. Exp. Immunol.* 1992. **90:** 330–335.

29 **Hirono, S., Islam, M. O., Nakazawa, M., Yoshida, Y., Kodama, M., Shibata, A., Izumi, T. and Imai, S.,** Expression of inducible nitric oxide synthase in rat experimental autoimmune myocarditis with special reference to changes in cardiac hemodynamics. *Circ. Res.* 1997. **80:** 11–20.

30 **Heim, A., Zeuke, S., Weiss, S., Ruschewski, W. and Grumbach, I. M.,** Transient induction of cytokine production in human myocardial fibroblasts by coxsackievirus B3. *Circ. Res.* 2000. **86:** 753–759.

31 **Morgan, M. P., Whelan, L. C., Sallis, J. D., McCarthy, C. J., Fitzgerald, D. J. and McCarthy, G. M.,** Basic calcium phosphate crystal-induced prostaglandin E2 production in human fibroblasts: role of cyclooxygenase 1, cyclooxygenase 2, and interleukin-1beta. *Arthritis Rheum.* 2004. **50:** 1642–1649.

32 **Eghbali, M., Czaja, M. J., Zeydel, M., Weiner, F. R., Zern, M. A., Seifter, S. and Blumenfeld, O. O.,** Collagen chain mRNAs in isolated heart cells from young and adult rats. *J. Mol. Cell. Cardiol.* 1988. **20:** 267–276.

33 **Westman, M., Korotkova, M., af Klint, E., Stark, A., Audoly, L. P., Klareskog, L., Ulfgren, A. K. and Jakobsson, P. J.,** Expression of microsomal prostaglandin E synthase 1 in rheumatoid arthritis synovium. *Arthritis Rheum.* 2004. **50:** 1774–1780.

34 **Gabay, C., Porter, B., Guenette, D., Billir, B. and Arend, W. P.,** Interleukin-4 (IL 4) and IL-13 enhance the effect of IL-1beta on production of IL-1 receptor antagonist by human primary hepatocytes and hepatoma HepG2 cells: differential effect on C-reactive protein production. *Blood* 1999. **93:** 1299–1307.

35 **Kolios, G., Rooney, N., Murphy, C. T., Robertson, D. A. and Westwick, J.,** Expression of inducible nitric oxide synthase activity in human colon epithelial cells: modulation by T lymphocyte derived cytokines. *Gut* 1998. **43:** 56–63.

36 **Saito, A., Okazaki, H., Sugawara, I., Yamamoto, K. and Takizawa, H.,** Potential action of IL-4 and IL-13 as fibrogenic factors on lung fibroblasts *in vitro*. *Int. Arch. Allergy Immunol.* 2003. **132:** 168–176.

37 **Maruyama, H., Higuchi, N., Nishikawa, Y., Hirahara, H., Iino, N., Kameda, S., Kawachi, H., Yaoita, E., Gejyo, F. and Miyazaki, J.,** Kidney-targeted naked DNA transfer by retrograde renal vein injection in rats. *Hum. Gene Ther.* 2002. **13:** 455–468.

38 **Hou, D., Maclaughlin, F., Thiesse, M., Panchal, V. R., Bekkers, B. C., Wilson, E. A., Rogers, P. I., Coleman, M. C. and March, K. L.,** Widespread regional myocardial transfection by plasmid encoding Del-1 following retrograde coronary venous delivery. *Catheter. Cardiovasc. Interv.* 2003. **58:** 207–211.

39 **Kodama, M., Matsumoto, Y., Fujiwara, M., Masani, F., Izumi, T. and Shibata, A.,** A novel experimental model of giant cell myocarditis induced in rats by immunization with cardiac myosin fraction. *Clin. Immunol. Immunopathol.* 1990. **57:** 250–262.

40 **Nishino, T., Kodaira, T., Shin, S., Imagawa, K., Shima, K., Kumahara, Y., Yanaihara, C. and Yanaihara, N.,** Glucagon radioimmunoassay with use of antiserum to glucagon C-terminal fragment. *Clin. Chem.* 1981. **27:** 1690–1697.

41 **Isenberg, G. and Klockner, U.,** Calcium tolerant ventricular myocytes prepared by preincubation in a "KB medium". *Pflugers Arch.* 1982. **395:** 6–18.

Effect of Hydrodynamics-Based Gene Delivery of Plasmid DNA Encoding Interleukin-1 Receptor Antagonist-Ig for Treatment of Rat Autoimmune Myocarditis

Possible Mechanism for Lymphocytes and Noncardiac Cells

Hui Liu, MD; Haruo Hanawa, MD; Tsuyoshi Yoshida, MD; Raafat Elnaggar, MD; Manabu Hayashi, MD; Ritsuo Watanabe, MD; Ken Toba, MD; Kaori Yoshida, BS; He Chang, MD; Yuji Okura, MD; Kiminori Kato, MD; Makoto Kodama, MD; Hiroki Maruyama, MD; Junichi Miyazaki, MD; Mikio Nakazawa, PhD; Yoshifusa Aizawa, MD

Background—Interleukin-1 (IL-1) is a powerful and important cytokine in myocarditis. The purpose of this study was to evaluate the effect and possible mechanism of hydrodynamics-based delivery of the IL-1 receptor antagonist (IL-1RA)-immunoglobulin (Ig) gene for treatment of rat experimental autoimmune myocarditis (EAM).

Methods and Results—On the day after immunization, rats were transfected with either pCAGGS encoding IL-1RA-Ig or pCAGGS encoding Ig alone. On day 17, IL-1RA-Ig gene therapy was effective in controlling EAM, as monitored by a decreased ratio of heart weight to body weight, reduced myocarditis areas, reduced gene expression of atrial natriuretic peptide in hearts, and improved cardiac function in echocardiographic and hemodynamic parameters. Examination of the expression of IL-1–related genes in purified cells from EAM hearts suggested that ectopic IL-1RA-Ig–acting target cells were $\alpha\beta$T cells and noncardiomyocytic noninflammatory cells such as fibroblasts, smooth muscle cells, and endothelial cells. Therefore, we examined the effect of serum containing IL-1RA-Ig on the expression of immune-relevant genes within noncardiomyocytic cells cultured from EAM hearts or concanavalin A–stimulated lymphocytes derived from lymph nodes in EAM-affected rats. The expression of immunologic molecules (prostaglandin E synthase, cyclooxygenase-2, and IL-1β) in cultivated noncardiomyocytic cells and Th1 cytokines (IL-2 and IFN-γ) in lymphocytes was significantly decreased by the serum containing IL-1RA-Ig.

Conclusions—EAM was suppressed by hydrodynamics-based delivery of plasmid DNA encoding IL-1RA-Ig. In addition, IL-1RA-Ig suppressed gene expression of prostaglandin synthases and IL-1 in noncardiomyocytic cells and Th1 cytokines in lymphocytes. (***Circulation.* 2005;111:1593-1600.**)

Key Words: cardiomyopathy, dilated ■ cytokines ■ sialoglycoproteins ■ myocarditis ■ prostaglandins

Rat experimental autoimmune myocarditis (EAM) resembles human giant cell myocarditis,[1] and recurrent forms lead to dilated cardiomyopathy.[2] Histopathological investigation showed that CD11b$^+$ cells (macrophages, dendritic cells, granulocytes) and CD4$^+$ T cells infiltrated the heart, which severely injured cardiomyocytes in the acute stage, followed by fibrosis in the heart.[3] Various cytokines have been found in EAM-affected hearts.[4]

Interleukin-1 (IL-1), formerly known as lymphocyte activating factor, is an important inflammatory cytokine produced by monocytes, macrophages, dendritic cells, B cells, or NK cells.[5,6] There are 2 structurally distinct forms of IL-1, IL-1α and IL-1β, which are both potent stimulators of target cells.[5,7] IL1-β, which has a signal peptide and is excreted from cells, is important for regional inflammation.[8] The IL-1 receptor (IL-1R) is divided into 2 structurally distinct forms, namely IL-1 receptor I (IL-1RI) and II (IL-1RII). IL-1RI expressed on T cells and fibroblasts among other cell types,[9] when bound to IL-1, forms heterocomplexes with IL-1 receptor accessory protein (IL-1Racp) and thereby transduces intracellular signals.[10] However, IL-1RII consisting of IL-1 binding portion, a single transmembrane region, and a shorter cytoplasmic domain cannot transduce signals and acts as a decoy target.[11] On the other hand, there are 2 structurally distinct forms of IL-1 receptor antagonist (IL-1RA) made by alternative splicing: secreted IL-1RA (sIL-1RA) and intracel-

Received May 26, 2004; revision received November 5, 2004; accepted November 10, 2004.

From the Divisions of Cardiology (H.L., H.H., T.Y., R.E., M.H., R.W., K.T., K.Y., H.C., Y.O., K.K., M.K., Y.A.) and Clinical Nephrology and Rheumatology (H.M.), Niigata University Graduate School of Medical and Dental Sciences, and Department of Medical Technology, School of Health Sciences, Faculty of Medicine (M.N.), Niigata University, Niigata, and Division of Stem Cell Regulation Research, Osaka University Medical School (J.M.), Suita, Japan.

Correspondence to H. Hanawa, Division of Cardiology, Niigata University Graduate School of Medical and Dental Sciences, 1-757 Asahimachi-dori, Niigata 951-8120, Japan. E-mail hanawa@med.niigata-u.ac.jp

Circulation is available at http://www.circulationaha.org

DOI: 10.1161/01.CIR.0000160348.75918.CA

lular IL-1RA (icIL-1RA).[12] IL-1RA functions as an antagonist by competitively binding to IL-1RI.[13,14] IL-1RA cannot transduce intracellular signals because it is unable to bind to IL-1Racp.[12,15] IL-1RA–based therapies are being evaluated for a variety of diseases.[16–18]

The purpose of the present study was to investigate whether IL-1RA transduction ameliorated EAM and by what mechanisms this therapy occurred. Hydrodynamics-based gene transfer via the rapid tail vein injection of a large volume is more efficient than delivery by intramuscular injection with electroporation.[19,20] This method can retrogradely deliver plasmid DNA predominantly into hepatocytes via hepatic vein. Moreover, chimeras with immunoglobulin (Ig) facilitate elevated concentration levels.[21] In this study, we examined the efficacy of hydrodynamics-based delivery of plasmid DNA encoding an IL-1RA-Ig chimera.

Methods

Animals

Seven-week-old male Lewis rats were purchased from Charles-River Laboratories, Japan (Atsugi, Kanagawa, Japan) and were maintained in our animal facilities. Throughout the studies, all the animals were treated in accordance with the guidelines for animal experiments as laid out by our institute.

Induction of EAM

Cardiac myosin was prepared from the ventricular muscle of porcine hearts as previously described.[1] To produce EAM, each rat was immunized on day 0 with 0.2 mL emulsion containing cardiac myosin with an equal volume of complete Freund's adjuvant by a single subcutaneous injection in both footpads.

In Vivo Treatment of EAM With Plasmid DNA Encoding IL-1RA-Ig Gene

Construction of Plasmid DNA for Gene Transfer

We first constructed the plasmid vector pCAGGS-Ig-glucagon (Glu)-tag, containing *Swa*I and *Not*I restriction sites, via polymerase chain reaction (PCR) amplification. For this purpose, initial PCR products were generated from rat spleen cDNA using KOD Plus DNA polymerase (Toyobo) and the following primers: 5′-gaGAATTCATTTAAATgagaGCGGCCGCcgtgcccagaaactgtg-3′ (contains both *Swa*I and *Not*I restriction sites) and 5′-tcaaccactgcacaaaatcttgggctttacccggagagtgggagagact-3′. The final PCR product inserts were then amplified from the diluted products of the first PCR reaction with the following primers: 5′-gaGAATTCATTTAAATgagaGCGGCCGCcgtgcccagaaactgtg-3′ (as before) and 5′-gagagagaGAATTCtcaggtattcatcaaccac-tgcacaaaattcttgggc-3′. Finalized PCR products were inserted into the pCAGGS vector using *Eco*RI sites. *Escherichia coli* JM109 competent cells were then transformed, and recombinant plasmids were isolated by use of a Quantum Prep Plasmid Maxiprep kit (Bio-Rad Laboratories). To construct the control plasmid, pCAGGS-rat signal peptide (SP)-Ig-Glu-tag, the SP region of secretory leukocyte protease inhibitor, was amplified from EAM heart cDNA with the primers 5′-gaGAATTCATTTAAATgaagtccagcggcctcttcccc-3′ and 5′-gcagcatcGCGGCCGCtccttccacactccagggtgccag-3′, followed by insertion into pCAGGS-Ig-Glu-tag using *Swa*I and *Not*I sites. To construct the pCAGGS-mouse IL-1RA-Ig-Glu-tag, mouse IL-1RA was amplified from mouse splenocyte cDNA using the primers 5′-gagaattcATTTAAATggaaatctgctggggaccctac-3′ and 5′-gcagcatc GCGGCCGCttggtcttcctggaagtagaact-3′, followed by insertion into pCAGGS-Ig-Glu-tag using *Swa*I and *Not*I sites. Recombinant plasmids were isolated as described above.

Plasmid DNA Injection Techniques

Nineteen rats were divided into 2 groups, the pCAGGS-IL-1RA-Ig group (IL-1RA-Ig group; n=10) and the pCAGGS-SP-Ig group (SP-Ig group; n=9). Rats were injected with 800 μg pCAGGS-mouse IL-1RA-Ig-Glu-tag or pCAGGS-SP-Ig-Glu-tag via the tail vein within 15 seconds (receiving ≈80 mL/kg body weight) on day 1.[19]

Plasmid Chimeric Glucagons-Tag Protein Measurement

Blood samples were taken on days 2, 5, 8, 12, and 17. Glucagon concentrations were measured with a glucagons radioimmunoassay kit (Daiichi Radioisotope Laboratories).[22] Chimeric protein concentrations in blood were calculated with Glu-tag.[23] To observe the relationship of them and gene expression in liver, the livers were harvested on days 2, 5, 8, 12, and 17 after injection of pCAGGS-IL-1RA-Ig-Glu-tag into normal rats (n=4, respectively), and transgene expressions were examined by real-time reverse-transcriptase (RT) PCR using the following primers: 5′-tctgactgaccgcgttactccca-3′ (726 to 748 bases in pCAGGS) and 5′-atcagtgatgttaacttcctccag-3′ (316 to 339 bases in mouse sIL-1RA).

Evaluation of Echocardiography and Hemodynamic Parameters

On day 17, echocardiography was performed with a 7.5-MHz probe (SSD-630, Aloka ECHO camera). Left ventricular (LV) internal diameter in end diastole and end systole, interventricular septal thickness, LV posterior wall thickness, pericardial effusion (PE) under LV posterior wall thickness, and LV fractional shortening were calculated from M-mode echocardiograms over 3 consecutive cardiac cycles.

The hemodynamic parameters were measured after echocardiography. Mean arterial pressure was recorded through a catheter introduced into the right femoral artery. Central venous pressure (was recorded through a catheter introduced into the confluence of the vena cava with the right jugular vein. A catheter-tip transducer was inserted into the left ventricle from the right carotid artery to measure the peak left ventricular pressure and left ventricular end-diastolic pressure. The rates of intraventricular pressure rise and decline (±dP/dt) were measured with a differential amplifier. Heart rate was calculated from ECGs. All hemodynamic parameters were recorded on a thermostylus recorder after a stabilizing period of 10 minutes.

Evaluation of Histopathology

Heart and body weights were measured, and the ratio of heart weight to body weight (g/g) was calculated. Several transverse sections were cut from the midventricle slice and stained with Azan-Mallory. The myocarditis area of each specimen was determined with a color image analyzer (Mac SCOPE version 2.6, Mitani Corp).

Measurement of Atrial Natriuretic Peptide mRNA Levels

To measure mRNA levels of atrial natriuretic peptide (ANP), a heart failure marker, total RNA was isolated from the apical one third of the heart on day 17. The absolute copy number of ANP mRNA was measured by quantitative real-time RT-PCR.

Gene Expression of IL-1 Family in EAM Hearts

To evaluate crosstalk between members of the IL-1 family, the mRNA levels of IL-1α, IL-1β, IL-1RI, IL-1RII, IL-1Racp, sIL-1RA, or total IL-1RA (sIL-1RA+icIL-1RA) in both isolated and purified cells from EAM hearts were measured. On day 18, cardiomyocytes and the other cells in the hearts of EAM rats were isolated after collagenase perfusion treatment for 20 minutes with a Langendorff apparatus as reported previously.[24,25] Isolated cells, while maintained in an isotonic buffer, were separated serially through stainless steel sieves into cardiomyocytes and the other cells. Because the inflammatory cells are almost $CD11b^+$ cells (macrophages/dendritic cells/granulocytes) and $\alpha\beta T$ cells,[3] the other cells without cardiomyocytes were separated into $\alpha\beta T$ cells, $CD11b^+$ cells, and noncardiomyocytic noninflammatory (NCNI) cells (mainly fibroblasts, smooth